Electronic Supplementary Material (ESI) for Catalysis Science & Technology.

Supplementary information

$Fe(CN)_5$@PILs derived N-doped porous carbon with FeC_xN_y active sites as a robust electrocatalyst for oxygen reduction reaction

Shao-hua Zhang, [#a] Yi-jing Gao, [#a] Shan Cheng, [a] Yi-long Yan, [a] Shi-Jie Zhang, [a] Gui-lin Zhuang, [a*] Sheng-wei Deng, [a] Zhong-zhe Wei, [a] Xing Zhong, [a] Jian-guo Wang[a*]

Structure Characterization

The morphologies of materials and elemental species were detected by High performance transmission electron microscopy (HR-TEM, Tecnai G2 F30) and scanning ekectron microscopy (SEM, Hitachi S4700). Powder X-ray diffraction (PXRD) were conducted by a panalytical X-pert pro diffractometer with Cu-Kα radiation. X-ray photoelectron spectroscopy (XPS) were measured by a Kratos AXIS Ultra DLD instruments with 300 W Al Ka radiation and C 1s peak at 284.5 eV as internal standard. The surfaces area of catalysts was recorded by the measuring nitrogen adsorption isothermal in a Surface properties analyser instrument (3Flex, Micromeritics). Raman spectra were obtained by a Renishaw 2000 model confocal microscopy Raman spectrometer.

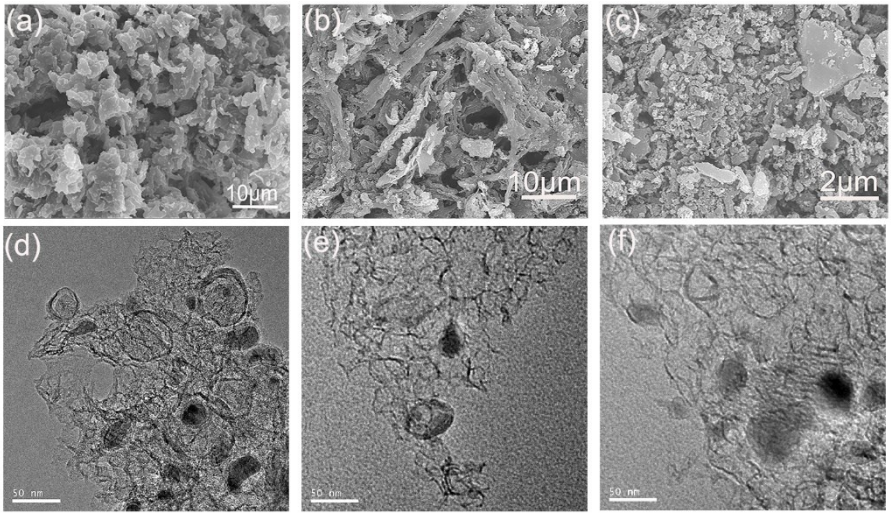

Fig. S1. (a-c), (d-f) are the SEM and TEM images of FeC_xN_y/N-PC-1, FeC_xN_y/N-PC-2 and FeC_xN_y/N-PC-4, respectively.

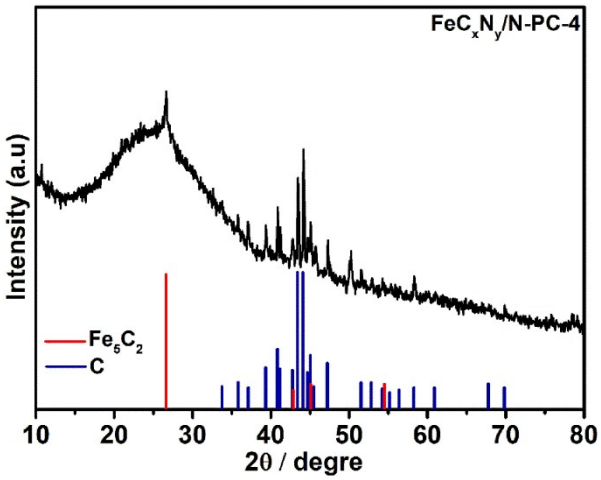

Fig. S2. XRD pattern of FeC_xN_y/N-PC-4 catalyst and Fe_5C_2 (JCPDS No. 51-0997), and C (JCPDS No. 01-0640).

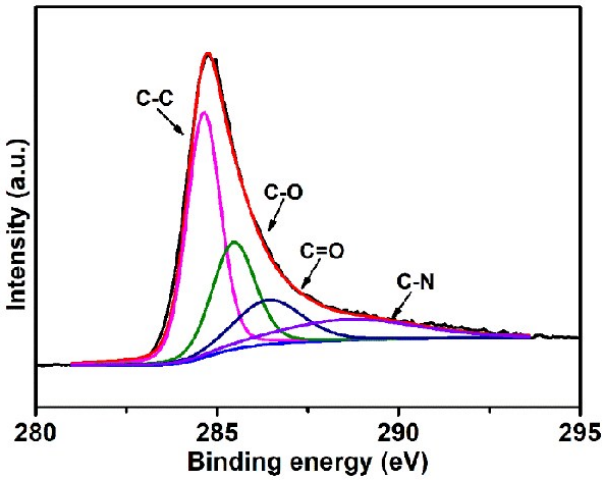

Fig. S3. High-resolution C 1s XPS spectra of FeC_xN_y/N-PC-3.

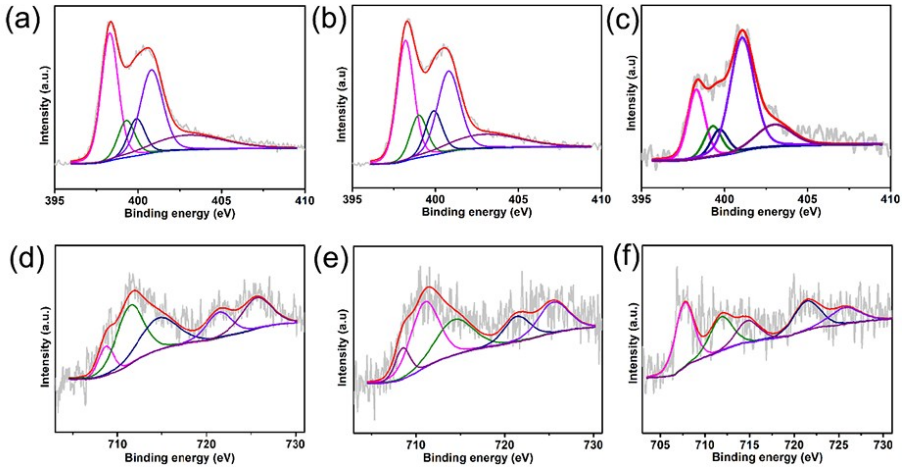

Fig. S4. High-resolution N 1s and Fe 2p XPS spectra of FeC_xN_y/N-PC-1, FeC_xN_y/N-PC-2 and FeC_xN_y/N-PC-4, respectively.

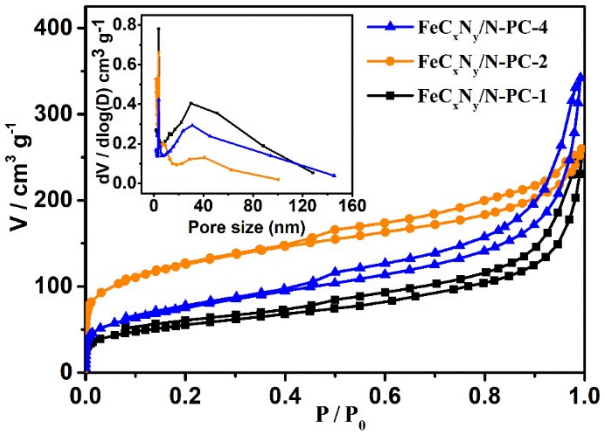

Fig. S5. Nitrogen adsorption-desorption isotherms and pore size distributions (inset) of FeC_xN_y/N-PC-1, FeC_xN_y/N-PC-2 and FeC_xN_y/N-PC-4.

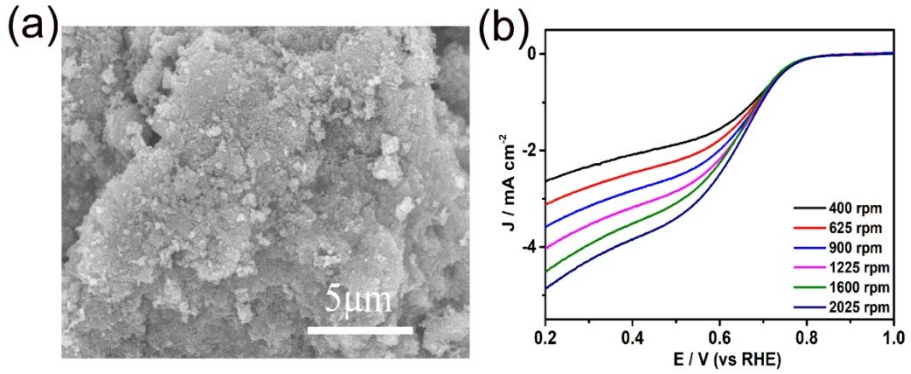

Fig. S6. (a-b) are the SEM image and LSVs of FeC_xN_y/N-PC, which was prepared without template.

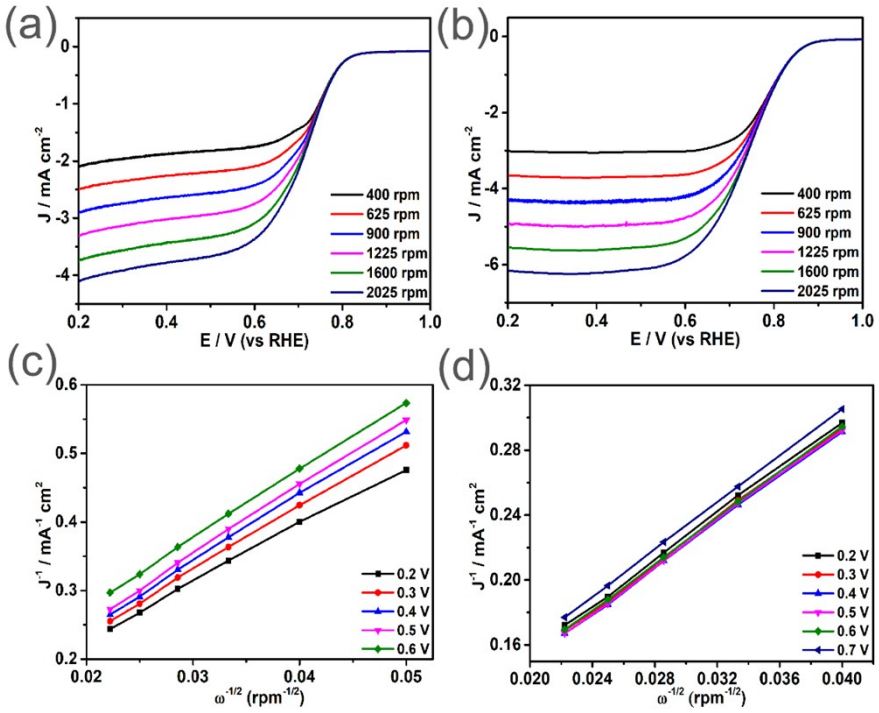

Fig. S7. (a-b) Polarization curve of C_xN_y and FeC_xN_y/N-PC-3, respectively. (c-d) show the Koutchy-Levich plots of catalysts at different potentials.

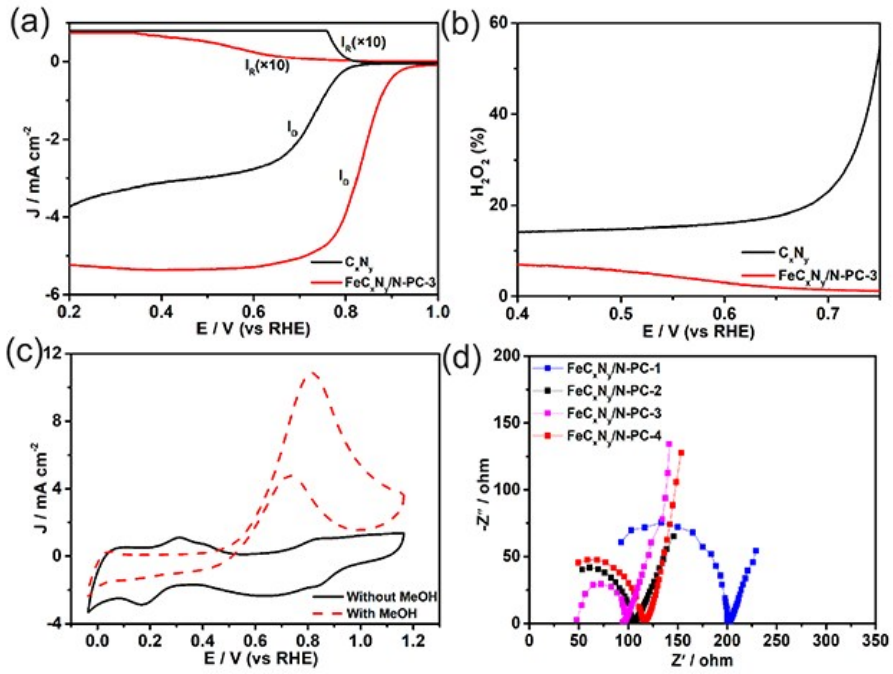

Fig. S8. (a) RRDE tests of C_xN_y and FeC_xN_y/N-PC-3 at 1600prm. (b) hydrogen peroxide yield of C_xN_y and FeC_xN_y/N-PC-3. (c) Pt/C in O_2-saturated 0.1 M KOH solution with and without MeOH with scan rate 50 mV/s. (d) Nyquist plot of EIS for ORR on FeC_xN_y/N-PC catalysts in 0.1M KOH solution. The inset corresponding equivalent circuit diagram of Nyquist plot of FeC_xN_y/N-PC. Rs, Rct and CPE are the electrolyte resistance, charge transfer resistance and constant phase element, respectively.

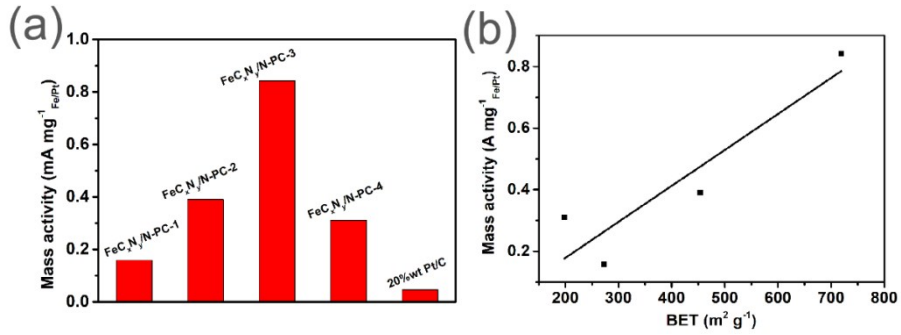

Fig. S9. Mass activity for these catalyst at 0.85 V vs RHE (a). Mass activity at 0.85 V vs BET for FeC_xN_y/N-PC.

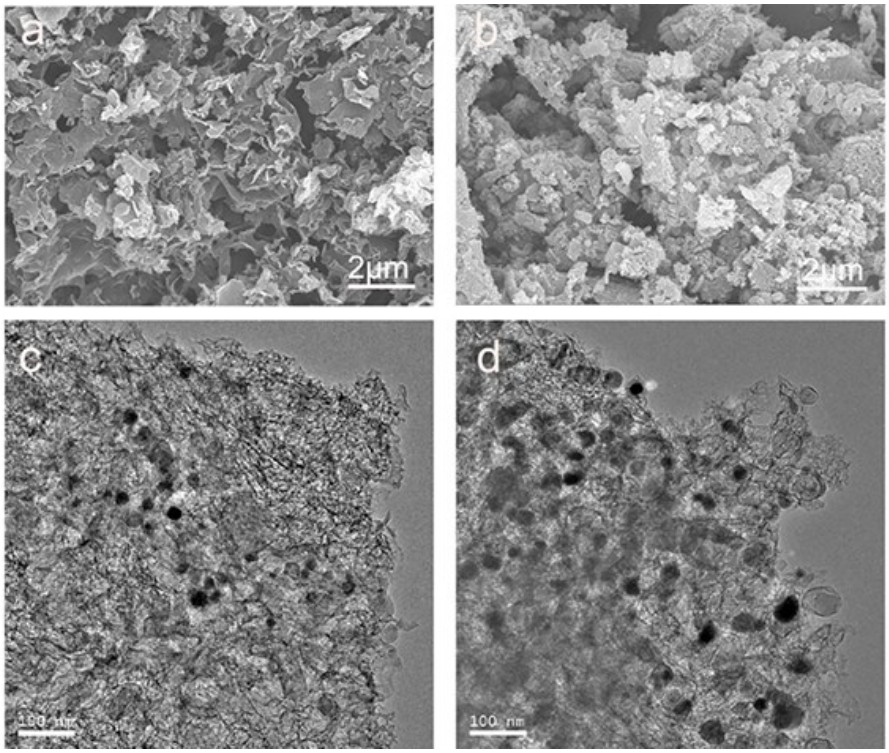

Fig. S10. (a-b) and (c-d) are the SEM and TEM images of FeC_xN_y/N-PC-0.5X and FeC_xN_y/N-PC-1.5X, respectively.

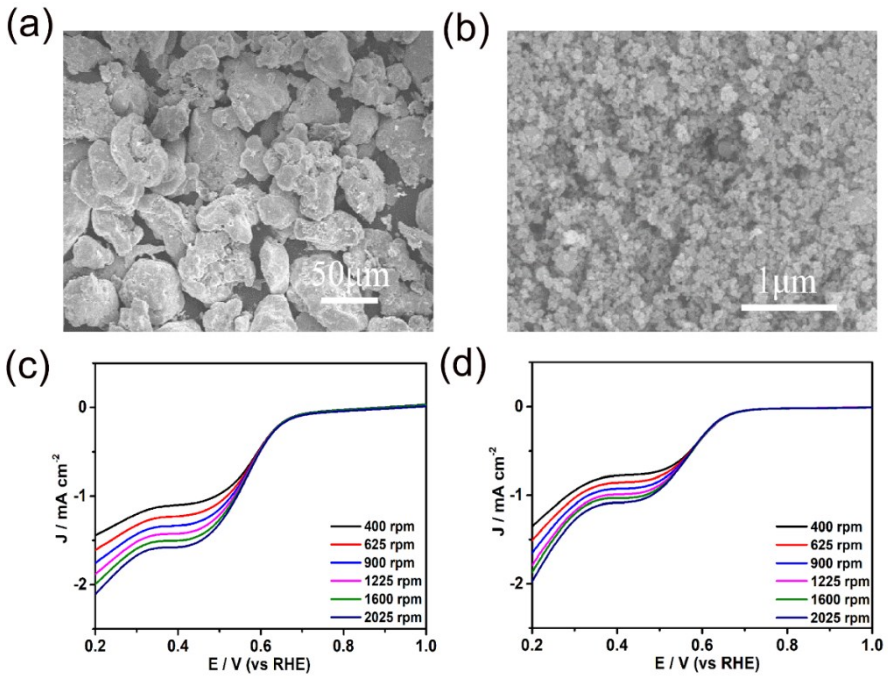

Fig. S11 (a-b) and (c-d) are the SEM images and LSVs of Fe_2O_3 and Fe_3C, respectively.

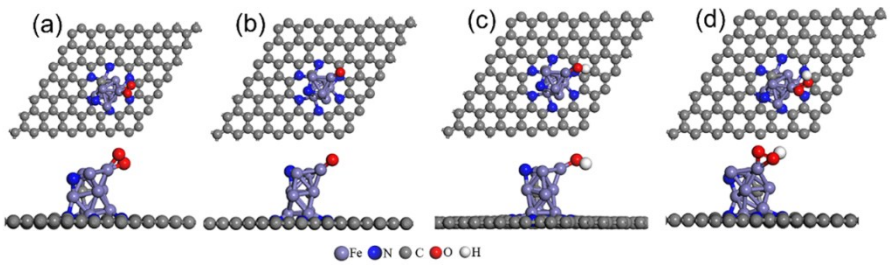

Fig. S12. Adsorption structure of O_2/ Fe_9CN@NPC (a), O/ Fe_9CN @NPC (b), OH/ Fe_9CN @NPC (c) and OOH/ Fe_9CN @NPC (d) on the T1site.

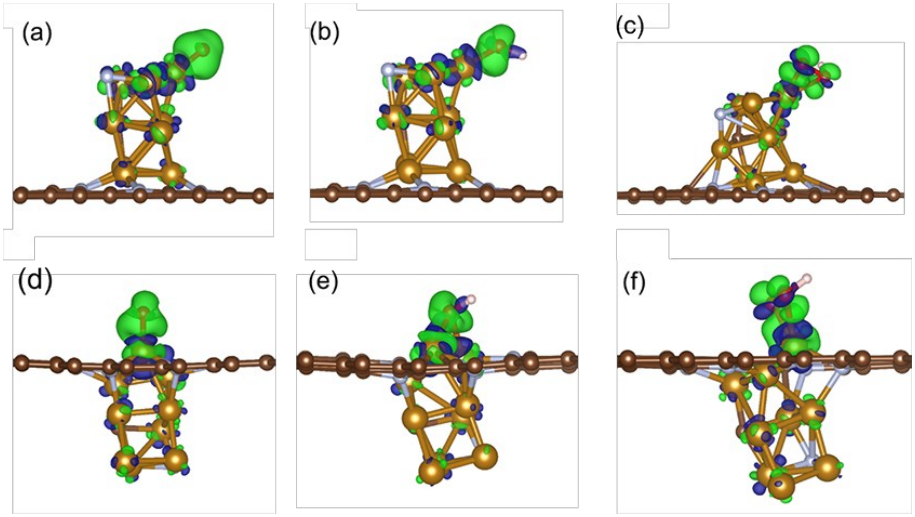

Fig. S13. Charge difference figure of adsorption configuration of reaction species on T2 (a – c) and H1 (e - h) site of Fe_9CN @NPC.

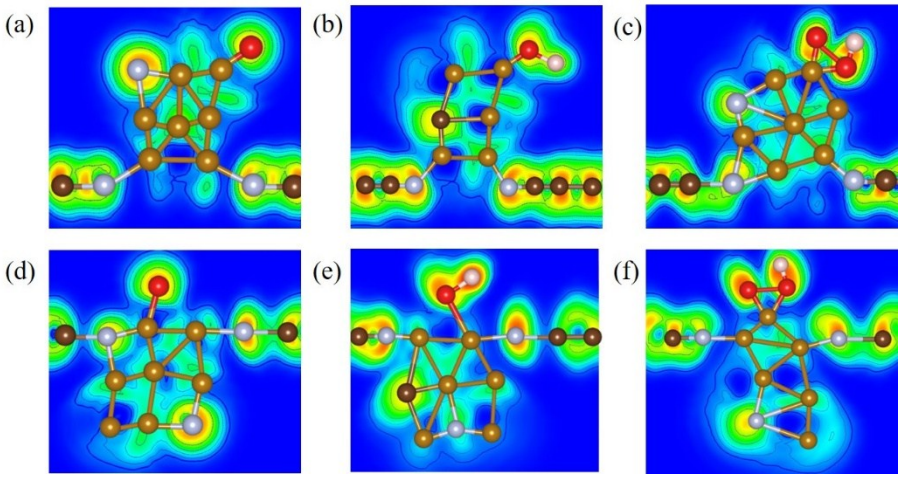

Fig. S14. Electron localization function plots for adsorption configuration of reaction species on T2 (a – c) and H1 (e - h) site of Fe_9CN @NPC.

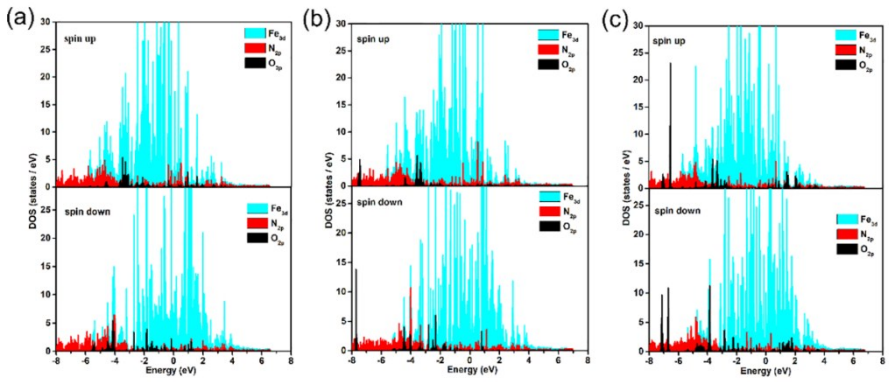

Fig. S15. Partial Density of state of Fe, O and N, O/ substrate (a), OH/ substrate (b) and OOH/ substrate (c) for the T2 active site.

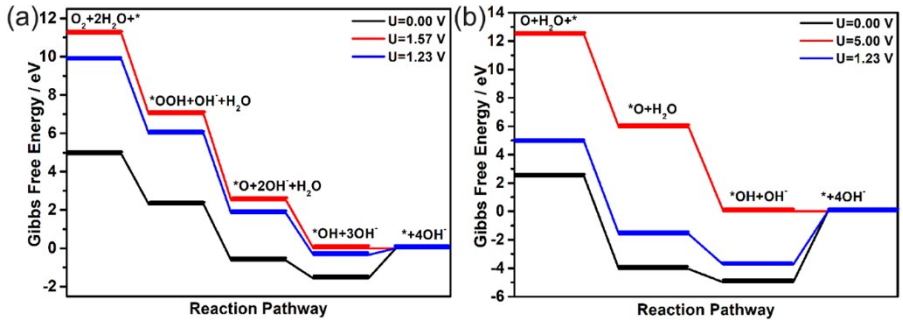

Fig. S16. Diagram of free energy of ORR on the T2 active site under association mechanism (a) and dissociation mechanism (b). pH=0.Black, red and blue lines represent reactions at zero electrode potential (U = 0 V), the over-potential and the equilibrium potential (U = 1.23 V), respectively.

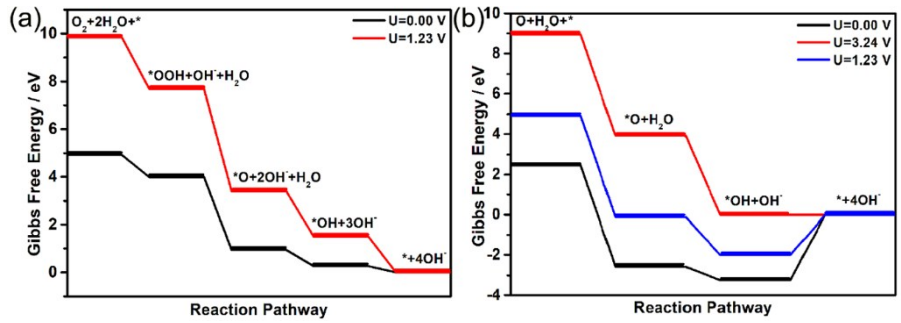

Fig. S17. Diagram of free energy of ORR on the H1 active site under association mechanism (a) and dissociation mechanism (b). pH=13.Black, red and blue lines represent reactions at zero electrode potential (U = 0 V), the over-potential and the equilibrium potential (U = 1.23 V), respectively.

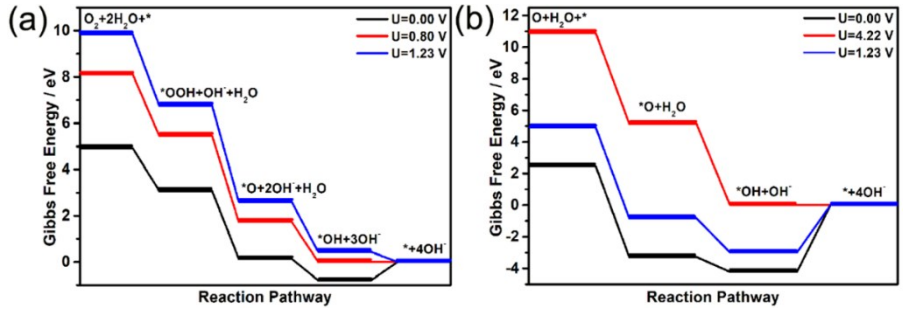

Fig. S18. Diagram of free energy of ORR on the T2 active site under association mechanism (a) and dissociation mechanism (b). pH=13.Black, red and blue lines represent reactions at zero electrode potential (U = 0 V), the over-potential and the equilibrium potential (U = 1.23 V), respectively.

Table S1. Textural properties of prepared catalysts.

Catalysts	Specific surface area ($m^2 g^{-1}$)	Pore volume ($cm^3 g^{-1}$)	Pore diameter (nm)
FeC_xN_y/N-PC-1	272.5	0.53	8.23
FeC_xN_y/N-PC-2	454.0	0.34	4.6
FeC_xN_y/N-PC-3	719.1	1.2	6.5
FeC_xN_y/N-PC-4	198.0	0.4	8.41

Table S2. XPS parameters for the catalysts. The atomic percentage content of catalysts and the percentage content of deconvoluted N-types.

catalysts	Fe	C	N	O	Py-N	Fe-N_x	Pyr-N	G-like	Py-N-O
FeC_xN_y/N-PC-1	0.76	80.36	11.15	7.73	34.2	9.8	9.9	29.6	16.5
FeC_xN_y/N-PC-2	1.01	81.48	10.06	7.45	32.3	11.4	11.8	28.8	15.7
FeC_xN_y/N-PC-3	0.95	83.02	9.15	6.88	24.0	10.1	13.6	31.8	20.5
FeC_xN_y/N-PC-4	0.78	89.24	3.82	6.16	20.9	9.2	7.8	48.3	13.8
FeC_xN_y/N-PC-0.5X	0.45	89.76	5.48	4.31	17.8	9.4	12.8	41.4	18.6
FeC_xN_y/N-PC-1.5X	1.21	79.95	9.48	9.36	32.2	13.0	12.2	32.2	10.4

Table S3. Comparison of the ORR performance for FeC_xN_y catalysts at 1600 rpm in 0.1 M KOH.

Catalysts	Loading mass (μg cm^{-2})	Half-wave potential (vs RHE)	Reference
FeC_xN_y/N-PC	160	0.84 V	This work
Fe-NMP	400	0.84 V	1
Fe_3C@C	300	0.80 V	2
MB-CFs	255	0.81 V	3
FeN_2/NOMC	510	0.86 V	4
Fe-N/HCN	100	0.85 V	5
C-FeZIF	500	0.86 V	6
Fe-NCA	200	0.81 V	7

Reference

1 M. M. Hossen, K. Artyushkova, P. Atanassov, A. Serov, *J. Power Sources*, 2018, **375**, 214-221.

2 A. Kong, Y. Zhang, Z. Chen, A. Chen, C. Li, H. Wang, Y. Shan, Carbon, 2017, **116**, 606-614.

3 C. Liu, J. Wang, J. Li, R. Luo, X. Sun, J. Shen, W. Han, L. Wang, *Carbon*, 2017, **114**, 706-716.

4 H. Shen, E. Gracia-Espino, J. Ma, H. Tang, X. Mamat, T. Wagberg, G. Hu, S. Guo, *Nano Energy*, 2017, **35**, 9-16.

5 Y. Wang, A. Kong, X. Chen, Q. Lin, P. Feng, *ACS Catal.*, 2015, **5**, 3887-3893.

6 Y. Deng, Y. Dong, G. Wang, K. Sun, X. Shi, L. Zheng, X. Li, S. Liao, *ACS Appl. Mater. Interfaces*, 2017, **9**, 9699-9709.

7 Q. Lai, Q. Gao, Q. Su, Y. Liang, Y. Wang, Z. Yang, *Nanoscale*, 2015, **7**, 14707-14714.